Acta Cryst. (1979). B35, 34–42

The Structure of Bytownite Quenched from 1723 K

BY A. FACCHINELLI, E. BRUNO AND G. CHIARI

Istituto di Mineralogia, Cristallografia e Geochimica dell'Università di Torino, Via San Massimo 24, I-10123 *Torino, Italy*

(*Received* 25 *July* 1978; *accepted* 6 *September* 1978)

Abstract

The structure of bytownite of composition An_{85} heated at 1723 K for 48 h, then quenched in air, has been refined in space group $I\bar{1}$. Two refinements were carried out: the first with only the non-tetrahedral cations considered as split half-atoms, and the remaining atoms treated anisotropically ($R = 0{\cdot}053$); the second with all split half-atoms (T and O atoms treated isotropically, $R = 0{\cdot}055$). The latter model has been chosen as the more realistic. On the basis of crystal-chemical criteria and by analogy with similar structures, a microdomain structure, compatible with the split model, is proposed. Compared to the low-temperature bytownite, the present structure shows a slightly larger Al/Si disorder in the single sites, but the same degree of Al concentration in the $T_1(0)$ average sites. This same concentration justifies the lack of variation of cell parameters between low and quenched bytownite. This concentration is correlated to the different bond-strength sums from the non-tetrahedral cations, and is interpreted in terms of charge balance. The role of tetrahedral linear distortion, as well as the different Al occupancy, in balancing the structure is pointed out.

Introduction

The structure of bytownite (body-centred anorthite) has been solved by Fleet, Chandrasekhar & Megaw (1966) who studied a low-temperature feldspar of composition $An_{80}Ab_{20}$. They showed the presence of antiphase microdomains, simulating the body-centred space group $I\bar{1}$, and of a nearly complete Al/Si ordered distribution. As part of a study on high-temperature calcic plagioclases, with the aim of clarifying the dependence of Al/Si order–disorder on the thermal treatment, the structure of a bytownite quenched from 1723 K is reported in this paper.

Experimental procedure

A sample of bytownite was taken from a satellite dyke of the Traversella stock (Sesia Lanzo zone, Western Alps). Isolated single crystals were heated at 1723 K for 48 h in an electric furnace, then quenched at room temperature. The chemical composition of the sample was checked (before and after the thermal treatment) by electron-microprobe analyses carried out in the wavelength-dispersion mode on a fully automated ARL–SEMQ instrument operated at 15 kV, 0·15 μA beam current and with a defocused beam (spot size 50 μm). Under these conditions no appreciable loss of Na counts was detected during three successive analyses on the same specimen point. Counting times were 2, 20 and 2 s for high background, peak and low background respectively. On-line data reduction was based on the Ziebold & Ogilvie (1964) method with the correction factors of Albee & Ray (1970). Synthetic plagioclases and natural microcline were used as standards for Si, Al, Ca, Na and K; natural olivine was used for Fe and Mg. The results shown in Table 1 confirm that the thermal treatment did not produce any significant chemical modification but a possible slight loss of Na. The chemical composition can be assumed to remain constant at ~ An_{85}.

The cell dimensions, before and after the thermal treatment, are listed in Table 2. They were obtained by

Table 1. *Chemical composition*

A: untreated; *B*: heated at 1723 K for 48 h and quenched. Analysts: R. Rinaldi and G. Vezzalini (University of Modena).

Chemical analyses (wt%)			Atomic proportions (O = 8)		
	A	*B*		*A*	*B*
CaO	17·33	17·13	Ca	0·85	0·85
Na_2O	1·62	1·25	Na	0·14	0·11
K_2O	0·06	0·16	K	–	0·01
MgO	0·05	0·03	Mg	–	–
FeO*	0·59	0·36	Fe	0·02	0·01
Al_2O_3	34·02	33·77	Al	1·83	1·84
SiO_2	47·21	46·67	Si	2·16	2·16
Total	100·88	99·37			

* All Fe as FeO.

0567-7408/79/010034-09$01.00

least squares from 46 and 39 reflections, respectively, measured on powder spectra obtained with a Guinier camera (internal standard correction was applied).

An untwinned quenched crystal was tested with long-exposure precession and Weissenberg photographs. It showed sharp '*a*' ($h + k$ = even, l = even) and '*b*' ($h + k$ = odd, l = odd) reflections, while the '*c*' ($h + k$ = even, l = odd) and '*d*' ($h + k$ = odd, l = even) were absent; therefore, the two possible space groups are $I\bar{1}$ and $I1$. The structure of a low-temperature bytownite (BytL hereinafter) (Fleet *et al.*, 1966) showed the presence of the same classes of reflections and has been proved to be centrosymmetric. As the loss of a centre of symmetry induced by heating is improbable, the space group of quenched bytownite (BytQ hereinafter) was assumed to be $I\bar{1}$.

The intensities were collected on a Philips PW 1100 four-circle diffractometer with graphite-monochromatized Mo radiation and the θ–2θ scan procedure. Both '*a*' and '*b*' reflections were kept on the same scale, but the weak '*b*' reflections were scanned eight times and then averaged to improve accuracy. Of the 3966 reflections measured, 1261 had $I/\sigma(I) \leq 1$ and were considered unobserved.* Of the 2705 reflections used in the refinement, 1731 were of '*a*' and 974 of '*b*' type. The absence of '*c*' and '*d*' reflections was also confirmed with the diffractometer by measuring a few reflections [the most intense among those listed by Foit & Peacor (1973)]. The measured intensities did not exceed background. Intensities were reduced in the conventional manner, although no absorption correction was applied. The crystal dimensions were 0·21 × 0·10 × 0·16 mm.

Table 2. *Cell parameters*

	Untreated	Quenched from 1723 K
a (Å)	8·188 (1)	8·183 (1)
b (Å)	12·882 (2)	12·883 (2)
c (Å)	14·196 (2)	14·186 (2)
α (°)	93·37 (2)	93·38 (2)
β (°)	116·04 (2)	115·87 (2)
γ (°)	90·87 (1)	90·82 (1)
U (Å^3)	1341·6	1341·9
$\Delta 2\theta^*_{(132-1\bar{3}2)}$ (°)	2·20	2·18

* Cu $K\alpha$ radiation.

Refinement of the structure

The refinement was carried out with a modified version of the *ORFLS* program (Busing, Martin & Levy, 1962) with the full-matrix approach. Scattering factors were taken from *International Tables for X-ray Crystallography* (1968). As a starting model, the average $I\bar{1}$ structure of BytL was chosen for T and O atoms. For Ca atoms, the split model of BytL, consisting of two half-atoms treated anisotropically, showed convergence at $R = 0{\cdot}053$. Table 3 lists the atomic coordinates and, for the Ca/Na atoms, the anisotropic thermal parameters of this refinement. The choice of the starting

* At the end of the refinement, one more cycle was performed with only those reflections for which $I > 3\sigma(I)$. The number of reflections so obtained was 2207. Almost all the 500 reflections with $1 < I/\sigma(I) \leq 3$ were of '*b*' type. As expected, R was slightly lower (0·051) and the atomic coordinates were the same, but the e.s.d.'s were larger. The '*b*' reflections are the only evidence of the doubling of the 7 Å cell; therefore, their presence in the refinement can reduce the effect of the pseudosymmetry vectors $(0,0,\frac{1}{2})$ and $(\frac{1}{2},\frac{1}{2},0)$. For this reason, these 500 reflections have been kept in the refinement in spite of their low intensities.

Table 3. *Atomic fractional coordinates* (×10^4) *and anisotropic thermal parameters* (×10^4) *of* Ca/Na *atoms in the non-split model*

	x	y	z	β_{11}	β_{22}	β_{33}	β_{12}	β_{13}	β_{23}	B (Å^2)
Ca/Na(000)	2670 (5)	9856 (4)	843 (3)	66 (6)	105 (4)	40 (2)	−28 (4)	19 (3)	−42 (3)	3·64
Ca/Na(0i0)	7753 (4)	5352 (2)	5443 (2)	42 (4)	21 (1)	12 (1)	8 (2)	4 (2)	−1 (1)	1·03
Ca/Na(z00)	2709 (7)	302 (3)	5453 (3)	47 (6)	23 (2)	16 (2)	12 (2)	8 (3)	−3 (1)	1·17
Ca/Na(zi0)	7632 (9)	5048 (7)	720 (5)	63 (7)	156 (8)	58 (5)	−16 (7)	22 (6)	−74 (4)	5·13
	x	y	z				x	y		z
T_1(0000)	73 (2)	1597 (1)	1050 (1)		O_B(0000)		8191 (6)	1010 (3)		922 (4)
T_1(0z00)	38 (2)	1639 (1)	6108 (1)		O_B(0z00)		8018 (7)	1022 (3)		5935 (4)
T_1(m000)	9 (2)	8151 (1)	1186 (1)		O_B(m000)		8096 (7)	8548 (4)		1252 (4)
T_1(mz00)	31 (2)	8169 (1)	6126 (1)		O_B(mz00)		8197 (7)	8553 (4)		6173 (4)
T_2(0000)	6870 (2)	1117 (1)	1590 (1)		O_C(0000)		125 (7)	2820 (3)		1374 (3)
T_2(0z00)	6792 (2)	1065 (1)	6583 (1)		O_C(0z00)		150 (6)	2932 (3)		6475 (3)
T_2(m000)	6772 (2)	8811 (1)	1804 (1)		O_C(m000)		95 (6)	6814 (3)		1078 (3)
T_2(mz00)	6828 (2)	8759 (1)	6777 (1)		O_C(mz00)		83 (6)	6896 (3)		6020 (3)
O_A(1000)	68 (7)	1265 (4)	9907 (3)		O_D(0000)		1939 (6)	1065 (4)		1877 (3)
O_A(1z00)	10 (7)	1260 (3)	4900 (3)		O_D(0z00)		2008 (6)	1040 (3)		6913 (3)
O_A(2000)	5765 (6)	9901 (3)	1395 (3)		O_D(m000)		1942 (6)	8676 (4)		2175 (4)
O_A(2z00)	5747 (6)	9909 (3)	6384 (3)		O_D(mz00)		1872 (7)	8625 (4)		7117 (4)

model consisting of non-split T and O atoms and split Ca atoms, made by analogy of the present refinement with those by Fleet *et al.* (1966) on BytL, by Bruno, Chiari & Facchinelli (1976) on quenched anorthite (AnQ hereinafter) and by Foit & Peacor (1973) on anorthite at high temperature, was proved to be correct by the low R obtained.

Table 4. *Root-mean-square displacements* ($\times 10^4$ Å)

	x	y	z		x	y	z
Ca/Na(000)	151	333	112	$O_A(2000)$	101	145	89
Ca/Na(0i0)	112	147	93	$O_A(2z00)$	121	139	103
Ca/Na(z00)	109	161	95	$O_B(0000)$	151	165	105
Ca/Na(zi0)	132	421	118	$O_B(0z00)$	127	186	105
$T_1(0000)$	95	128	87	$O_B(m000)$	147	214	128
$T_1(0z00)$	91	120	64	$O_B(mz00)$	163	204	112
$T_1(m000)$	97	113	59	$O_C(0000)$	126	165	115
$T_1(mz00)$	104	123	84	$O_C(0z00)$	141	157	81
$T_2(0000)$	92	112	87	$O_C(m000)$	130	165	119
$T_1(0z00)$	98	122	97	$O_C(mz00)$	118	164	94
$T_2(m000)$	102	115	92	$O_D(0000)$	148	164	100
$T_2(mz00)$	96	109	67	$O_D(0z00)$	133	183	100
$O_A(1000)$	159	180	75	$O_D(m000)$	131	231	85
$O_A(1z00)$	138	183	87	$O_D(mz00)$	159	226	127

The next step was the refinement of a complete split-atom structure. It was carried out following the refinement of the AnQ structure exactly (Bruno *et al.*, 1976). All the T and O atoms, which mainly had elongated thermal ellipsoids (Table 4), have been transformed into pairs of half-atoms symmetrically located with respect to the barycentre of the ellipsoid (Bruno *et al.*, 1976). Full-matrix refinement with anisotropic thermal parameters for Ca and isotropic for T and O atoms led to an R of 0·055. For the same reasons given in the discussion of BytL and AnQ the half-atom split model is assumed to be more realistic, and the discussion which follows deals with this model only.*

Choice of a whole-atom structure

In low-temperature anorthite (AnWS hereinafter) the presence of 'c' and 'd' reflections leads to the space

* Lists of structure factors for both models and anisotropic thermal parameters for the O and T atoms of the non-split model have been deposited with the British Library Lending Division as Supplementary Publication No. SUP 33891 (22 pp.). Copies may be obtained through The Executive Secretary, International Union of Crystallography, 5 Abbey Square, Chester CH1 2HU, England.

Table 5. *Atomic fractional coordinates* ($\times 10^4$), *anisotropic thermal parameters* ($\times 10^4$) *of* Ca/Na *atoms and isotropic thermal parameters of* T *and* O *atoms in the* $P\bar{1}$ *model*

	x	y	z	β_{11}	β_{22}	β_{33}	β_{12}	β_{13}	β_{23}	B(Å^2)
Ca/Na(000)	2665 (5)	9858 (4)	842 (3)	66 (6)	109 (4)	39 (2)	−26 (4)	19 (3)	−41 (3)	3·71
Ca/Na(0i0)	7751 (4)	5352 (2)	5442 (2)	47 (4)	23 (1)	12 (1)	9 (2)	4 (2)	−2 (1)	1·10
Ca/Na(z00)	2715 (7)	306 (3)	5455 (3)	42 (6)	20 (1)	15 (2)	11 (2)	8 (2)	−2 (1)	1·08
Ca/Na(zi0)	7631 (9)	5040 (7)	721 (5)	66 (7)	148 (8)	60 (5)	−24 (7)	26 (6)	−73 (5)	5·05

	x	y	z	B (Å^2)		x	y	z	B (Å^2)
$T_1(0000)$	4 (9)	1656 (5)	1056 (5)	1·13 (15)	$O_B(0000)$	8109 (22)	1025 (12)	849 (12)	1·29 (31)
$T_1(00i0)$	5124 (7)	6548 (4)	6044 (4)	0·25 (11)	$O_B(00i0)$	3268 (22)	5996 (13)	5990 (12)	1·51 (32)
$T_1(0z00)$	137 (8)	1602 (5)	6118 (5)	0·48 (13)	$O_B(0z00)$	8162 (17)	971 (9)	6027 (9)	1·09 (22)
$T_1(0zi0)$	4944 (8)	6677 (5)	1099 (5)	0·42 (12)	$O_B(0zi0)$	2896 (16)	6071 (9)	852 (9)	1·01 (22)
$T_1(m000)$	9938 (9)	8100 (5)	1172 (5)	0·47 (15)	$O_B(m000)$	8179 (18)	8509 (10)	1368 (10)	1·93 (23)
$T_1(m0i0)$	5075 (9)	3202 (5)	6199 (6)	0·52 (15)	$O_B(m0i0)$	3026 (16)	3579 (9)	6147 (9)	1·33 (21)
$T_1(mz00)$	96 (10)	8206 (5)	6130 (6)	0·51 (15)	$O_B(mz00)$	8100 (16)	8552 (9)	6070 (9)	1·22 (21)
$T_1(mzi0)$	4966 (10)	3128 (6)	1122 (6)	0·93 (17)	$O_B(mzi0)$	3308 (18)	3556 (10)	1293 (10)	1·80 (24)
$T_2(0000)$	6926 (10)	1102 (6)	1567 (6)	0·53 (16)	$O_C(0000)$	9992 (18)	2876 (10)	1334 (10)	1·26 (26)
$T_2(00i0)$	1815 (11)	6127 (6)	6615 (6)	0·67 (17)	$O_C(00i0)$	5243 (17)	7777 (10)	6411 (10)	0·83 (24)
$T_2(0z00)$	6753 (10)	1073 (5)	6612 (6)	0·53 (15)	$O_C(0z00)$	238 (21)	2892 (11)	6439 (12)	1·50 (31)
$T_2(0zi0)$	1834 (10)	6059 (6)	1547 (6)	1·03 (17)	$O_C(0zi0)$	5083 (18)	7964 (10)	1507 (11)	0·82 (24)
$T_2(m000)$	6735 (11)	8829 (6)	1831 (6)	0·76 (18)	$O_C(m000)$	42 (20)	6772 (11)	1113 (11)	1·29 (28)
$T_2(m0i0)$	1807 (11)	3792 (6)	6777 (6)	0·76 (18)	$O_C(m0i0)$	5160 (21)	1859 (11)	6042 (12)	1·34 (29)
$T_2(mz00)$	6883 (10)	8734 (6)	6757 (6)	0·58 (16)	$O_C(mz00)$	205 (18)	6947 (10)	5997 (10)	1·22 (26)
$T_2(mzi0)$	1776 (10)	3785 (6)	1798 (6)	0·47 (16)	$O_C(mzi0)$	4975 (15)	1854 (8)	1041 (8)	0·49 (19)
$O_A(1000)$	251 (19)	1303 (10)	9953 (11)	1·29 (26)	$O_D(0000)$	1846 (18)	1092 (10)	1925 (10)	1·19 (25)
$O_A(10i0)$	4905 (18)	6234 (9)	4868 (10)	0·87 (22)	$O_D(00i0)$	7023 (17)	6047 (10)	6831 (10)	0·96 (23)
$O_A(1z00)$	9854 (19)	1263 (10)	4872 (10)	1·02 (24)	$O_D(0z00)$	2095 (17)	1055 (10)	6871 (10)	1·03 (22)
$O_A(1zi0)$	5192 (19)	6264 (10)	9936 (11)	1·34 (26)	$O_D(0zi0)$	6909 (18)	6016 (10)	1959 (10)	1·36 (25)
$O_A(2000)$	5682 (19)	9926 (11)	1430 (11)	0·85 (28)	$O_D(m000)$	2031 (13)	8704 (7)	2094 (7)	0·71 (15)
$O_A(20i0)$	835 (18)	4875 (10)	6359 (10)	0·69 (26)	$O_D(m0i0)$	6827 (14)	3643 (8)	7267 (8)	1·38 (19)
$O_A(2z00)$	5753 (20)	9870 (11)	6326 (11)	1·00 (29)	$O_D(mz00)$	1766 (16)	8584 (9)	7174 (9)	1·37 (20)
$O_A(2zi0)$	747 (20)	4947 (11)	1442 (11)	0·88 (28)	$O_D(mzi0)$	7000 (17)	3664 (9)	2056 (10)	1·89 (22)

group $P\bar{1}$. Megaw, Kempster & Radoslovich (1962) and Wainwright & Starkey (1971) were therefore able to refine the structure in a straightforward manner. Diffraction data on samples of pure anorthite collected at a temperature above 500 K (Foit & Peacor, 1973; Czank, 1973) or collected at room temperature on samples quenched from a temperature near the melting point (Bruno *et al.*, 1976) showed the disappearance of the '*c*' and '*d*' reflections. The low-temperature bytownite, even at room temperature, does not show the '*c*' and '*d*' reflections. To interpret this lack, Fleet *et al.* (1966) proposed a model based on the presence of antiphase $P\bar{1}$ microdomains related by the vector (**a** + **b** + **c**)/2. The presence of antiphase domains has been confirmed by electron-microscope observations. All the above-mentioned authors agreed in extending to heated anorthite the space-average model proposed by Fleet *et al.* (1966).

In the present work also, the hypothesis of antiphase $P\bar{1}$ microdomains has been accepted and the same procedure as applied to the AnQ structure has been followed in choosing a whole-atom structure compatible with the half-atom split model. The criteria for choosing one of the 2^{25} possible $P\bar{1}$ configurations compatible with the $I\bar{1}$ split model are based on plausibility of coordination and of bond lengths and on the analogy between BytQ and BytL, AnQ, AnWS. These criteria can help in excluding many con-

Table 6. Ca/Na–O *interatomic distances* (Å)

	Ca/Na(000)			Ca/Na(0*i*0)			Ca/Na(*z*00)			Ca/Na(*zi*0)	
	BytQ	BytL		BytQ	BytL		BytQ	BytL		BytQ	BytL
O_A(1000)	2·677	2·669	O_A(10*i*0)	2·430	2·439	O_A(1*z*00)	2·490	2·434	O_A(1*zi*0)	2·463	2·387
O_A(100*c*)	2·560	2·526	O_A(10*ic*)	2·833	2·845	O_A(1*z*0*c*)	2·764	2·853	O_A(1*zic*)	2·618	2·727
O_A(2000)	2·233	2·304	O_A(20*i*0)	2·390	2·312	O_A(2*z*00)	2·337	2·361	O_A(2*zi*0)	2·304	2·331
O_A(2*z*0*c*)	3·636*	3·527*	O_A(20*ic*)	3·233*	3·308*	O_A(2*z*0*c*)	3·272*	3·310*	O_A(20*ic*)	3·762*	3·956*
O_A(200*c*)	>4*	3·998*							O_A(2*zic*)	3·839*	3·551*
O_B(000*c*)	2·406	2·407	O_B(00*ic*)	2·430	2·413	O_B(0*z*0*c*)	2·426	2·484	O_B(0*zic*)	2·445	2·388
O_B(*m*00*c*)	3·697*	3·769*	O_B(*m*0*ic*)	2·554	2·627	O_B(*mz*0*c*)	2·537	2·419	O_B(*mzic*)	3·280*	2·976
O_C(0*zi*0)	3·089	3·047	O_C(0*z*00)	3·793*	3·676*	O_C(00*i*0)	3·873*	3·834*	O_C(0000)	3·352*	3·612*
O_C(*mzi*0)	3·094*	3·302*	O_C(*mz*00)	2·680	2·609	O_C(*m*0*i*0)	2·634	2·500	O_C(*m*000)	2·820	2·707
O_D(0000)	2·445	2·447	O_D(00*i*0)	2·422	2·422	O_D(0*z*00)	2·429	2·455	O_D(0*zi*0)	2·384	2·422
O_D(*m*000)	2·593	2·565	O_D(*m*0*i*0)	3·802*	3·697*	O_D(*mz*00)	3·703*	3·844*	O_D(*mzi*0)	2·866	3·095*

* Assumed to be non-bonded.

Table 7. T–O *bond lengths* (Å) *and* Δ_{tet} ($\times 10^2$)

T_1(0000)–O_A(1000)	1·700	T_1(*m*000)–O_A(1000)	1·760	T_2(0000)–O_A(2000)	1·766	T_2(*m*000)–O_A(2000)	1·663
O_B(0000)	1·640	O_B(*m*000)	1·668	O_B(0000)	1·684	O_B(*m*000)	1·629
O_C(0000)	1·600	O_C(*m*000)	1·713	O_C(*mzi*0)	1·770	O_C(0*zi*0)	1·623
O_D(0000)	1·684	O_D(*m*000)	1·771	O_D(*mz*00)	1·653	O_D(0*z*00)	1·659
Mean	1·656	Mean	1·728	Mean	1·718	Mean	1·644
Δ_{tet}	0·056	Δ_{tet}	0·056	Δ_{tet}	0·088	Δ_{tet}	0·012
T_1(00*i*0)–O_A(10*i*0)	1·624	T_1(*m*0*i*0)–O_A(10*i*0)	1·723	T_2(00*i*0)–O_A(20*i*0)	1·737	T_2(*m*0*i*0)–O_A(20*i*0)	1·627
O_B(00*i*0)	1·637	O_B(*m*0*i*0)	1·724	O_B(00*i*0)	1·772	O_B(*m*0*i*0)	1·621
O_C(00*i*0)	1·624	O_C(*m*0*i*0)	1·738	O_C(*mz*00)	1·661	O_C(0*z*00)	1·606
O_D(00*i*0)	1·636	O_D(*m*0*i*0)	1·628	O_D(*mzi*0)	1·704	O_D(0*zi*0)	1·636
Mean	1·630	Mean	1·703	Mean	1·718	Mean	1·622
Δ_{tet}	0·001	Δ_{tet}	0·066	Δ_{tet}	0·057	Δ_{tet}	0·005
T_1(0*z*00)–O_A(1*z*00)	1·708	T_1(*mz*00)–O_A(1*z*00)	1·629	T_2(0*z*00)–O_A(2*z*00)	1·683	T_2(*mz*00)–O_A(2*z*00)	1·738
O_B(0*z*00)	1·749	O_B(*mz*00)	1·666	O_B(0*z*00)	1·691	O_B(*mz*00)	1·681
O_C(0*z*00)	1·688	O_C(*mz*00)	1·630	O_C(*m*0*i*0)	1·611	O_C(00*i*0)	1·694
O_D(0*z*00)	1·683	O_D(*mz*00)	1·558	O_D(*m*000)	1·668	O_D(0000)	1·695
Mean	1·707	Mean	1·621	Mean	1·663	Mean	1·702
Δ_{tet}	0·023	Δ_{tet}	0·058	Δ_{tet}	0·035	Δ_{tet}	0·016
T_1(0*zi*0)–O_A(1*zi*0)	1·799	T_1(*mzi*0)–O_A(1*zi*0)	1·690	T_2(0*zi*0)–O_A(2*zi*0)	1·640	T_2(*mzi*0)–O_A(2*zi*0)	1·720
O_B(0*zi*0)	1·719	O_B(*mzi*0)	1·579	O_B(0*zi*0)	1·574	O_B(*mzi*0)	1·715
O_C(0*zi*0)	1·710	O_C(*mzi*0)	1·639	O_C(*m*000)	1·643	O_C(0000)	1·720
O_D(0*zi*0)	1·803	O_D(*mzi*0)	1·714	O_D(*m*0*i*0)	1·576	O_D(00*i*0)	1·754
Mean	1·756	Mean	1·655	Mean	1·606	Mean	1·727
Δ_{tet}	0·061	Δ_{tet}	0·098	Δ_{tet}	0·043	Δ_{tet}	0·008

figurations, but do not point to a unique solution. Starting from the Ca atoms, unambiguously assigned as 0 or *i*, it was possible, however, to identify all O and T atoms except $O_C(0000) - O_C(00i0)$ and $T_1(0000) - T_1(00i0)$. For these two pairs an arbitrary choice was made. The alternative choices, however, would not significantly change the bond distances, upon which the discussion to follow is centred. There are many possible $P\bar{1}$ configurations, and that shown in Table 5 is simply one of the most probable. Tables 6, 7, 8 and 9 show the Ca–O and T–O distances, and the O–T–O and T–O–T angles. E.s.d.'s are 0·013 and 0·018 Å for Ca–O and T–O bonds, respectively, and 0·9° for O–T–O and T–O–T angles.

Discussion

Ca/Na *environment*

Table 6 shows the Ca/Na–O distances up to 4 Å for both BytQ and BytL. There is good agreement between the two sets. The only discrepancy concerns $O_B(mzic)$ and $O_D(mzi0)$, both surrounding the Ca/Na($zi0$) atom. Fixing at 3 Å the limit of the coordination sphere, $O_B(mzic)$ is Ca/Na coordinated in BytL (2·976 Å) but not in BytQ (3·280 Å). The contrary is true for $O_D(mzi0)$ (3·095 and 2·866 Å respectively). The Ca–O distances found in BytQ for these two atoms are closer to those found in both AnWS and AnQ (3·301 and 3·192 Å for O_B; 2·715 and 2·961 Å for O_D, respectively). These two atoms are approximately located along the longest axis of the very large thermal ellipsoid of Ca/Na($zi0$) and have two of the highest temperature factors (1·80 for O_B and 1·89 Å^2 for O_D). The difference in the Ca/Na($zi0$) coordination between BytL and BytQ can be ascribed to a different location of the Ca/Na atom along the direction of the major axis of the thermal ellipsoid rather than to a different shape of the cavity. This is in agreement with the fact that the mean Ca/Na($zi0$)–O distances are almost equal in the two structures (2·563 for BytL and 2·557 Å for BytQ).

Table 8. *Bond angles at* T (°)

	O_A–O_B	O_A–O_C	O_A–O_D	O_B–O_C	O_B–O_D	O_C–O_D
$T_1(0000)$	102·6	116·8	97·9	113·2	112·0	113·1
$T_1(00i0)$	101·0	118·1	105·0	109·8	115·4	107·7
$T_1(0z00)$	97·8	115·7	103·0	112·8	115·4	111·3
$T_1(0zi0)$	101·5	121·5	93·8	112·9	114·5	111·2
$T_1(m000)$	104·8	115·6	98·8	113·0	112·4	111·4
$T_1(m0i0)$	101·7	109·8	109·8	112·5	113·6	109·2
$T_1(mz00)$	102·7	109·9	111·4	112·2	114·3	106·3
$T_1(mzi0)$	102·5	117·0	100·2	113·1	111·8	111·3
$T_2(0000)$	111·3	94·4	109·5	114·5	112·6	113·1
$T_2(00i0)$	100·2	108·7	107·2	109·8	112·1	117·4
$T_2(0z00)$	101·2	106·3	110·3	111·6	109·7	116·6
$T_2(0zi0)$	113·8	96·8	110·0	113·0	110·1	112·8
$T_2(m000)$	115·6	103·8	109·0	112·9	106·3	109·2
$T_2(m0i0)$	104·4	107·8	107·9	109·8	111·0	115·2
$T_2(mz00)$	104·7	106·0	108·2	110·4	114·2	112·7
$T_2(mzi0)$	111·9	104·0	104·1	113·1	108·2	115·2

Table 9. *Bond angles at* O (°)

O_A		O_B	O_C	O_D
1000	136·7	0000	128·7	128·6	134·2
10i0	140·5	00i0	139·2	133·6	129·5
1z00	139·9	0z00	138·1	133·6	128·5
1zi0	133·7	0zi0	130·1	130·1	130·9
2000	121·0	m000	166·9	129·1	140·1
20i0	128·5	m0i0	147·3	131·9	163·0
2z00	124·8	mz00	145·0	132·9	161·7
2zi0	124·5	mzi0	162·4	125·8	140·5

Ca/Na *thermal parameters*

A typical feature of the calcic plagioclases, particularly evident in BytQ, is that the thermal parameters of the non-tetrahedral cations in the (000) and ($zi0$) sites are much larger than those in the ($0i0$) and ($z00$) sites. This is mainly due to the elongated shape of the Ca/Na(000) and Ca/Na($zi0$) thermal ellipsoids. The isotropic B's of BytQ, calculated as the average of the B_{ii} of the anisotropic refinement for the Ca/Na atoms, are in general larger than those in similar structures. (This can be only partially explained by the use of scattering factors for Ca neutral atoms not corrected for the presence of Na.) The differences in (000) and ($zi0$) sites compared to ($0i0$) and ($z00$) follow, however, the same trend as in the other structures. The main physical interpretations of the peculiarities presented by the thermal parameters of the large cations in this kind of structure, already discussed by other authors, are: (i) there is anisotropic thermal motion about a single node; (ii) the ellipsoids are a consequence of a statistical spatial disorder (multinode model) of the atoms around the average position; (iii) in those structures where there is a partial substitution Ca/Na, Na atoms are preferentially located in the (000) and ($zi0$) sites; (iv) in the same kind of structures as in (iii) there is a superposition of two or more different subcells or domains, with different chemical composition and with slightly different atomic positions; (v) there is a different atomic occupancy of the four sites.

Hypotheses (i), (ii) and (iv) can also explain the marked anisotropy of the (000) and ($zi0$) sites, while the other two only justify the difference between the isotropic B values of the two pairs of sites. The five hypotheses are not mutually exclusive, but can cooperate in explaining the thermal parameters of these atoms. In favour of (i), Jagodzinski & Kalus (1977) showed

that for pure $P\bar{1}$ low anorthite at very low temperature (55 K) all four sites show identical temperature factors.

The quenchability of the increase of thermal parameters induced by severe heating in AnQ when compared with AnWS (and possibly in BytQ, even though the thermal parameters for BytL were not refined) strongly supports hypothesis (ii) for quenched structures. The large temperature factors at room temperature after quenching could be reasonably interpreted as the freezing-in of a multinode model (average in space) of the large anisotropic thermal motion (average in time) possible at very high temperature.

It seems necessary to make a clear distinction between the low-temperature structures and those quenched from very high temperatures. This distinction recalls the two different interpretations of the Na anisotropy in low and high albite (Winter, Ghose & Okamura, 1977). These authors showed that the temperature factors of low albite decrease linearly with a decrease of temperature, and could be extrapolated to zero for $T = 0$ K. This fact is consistent with real thermal motion. For high albite, on the other hand, the B value extrapolated at $T = 0$ K is 6 Å^2. This proves the presence of a space average of the Na atom in high albite.

Similar data for the structures of anorthite and bytownite would be of great help in choosing between the first two hypotheses.

Hypotheses (iii) and (iv) are applicable only to Na-containing structures and do not explain the behaviour of pure anorthite. Hypothesis (v) is not compatible with a truly $P\bar{1}$ structure (as AnWS), but is compatible with those quenched structures in which the lack of 'c' and 'd' reflections is attributed to the presence of antiphase microdomains. In this case the $I\bar{1}$ situations occurring at the boundaries between the antiphase $P\bar{1}$ microdomains can favour a prevalence of left or right atoms (see Fig. 2 and discussion in Bruno *et al.*, 1976).

Apart from the various possible physical interpretations, it seems reasonable to correlate the differences among the thermal parameters of the four Ca/Na atoms in BytQ with geometrical differences of the corresponding cavities. If a seven-coordination model is assumed for all four sites, the average Ca/Na–O distance is larger for the (000) and ($zi0$) sites (2·572 and 2·557 Å) than for the ($0i0$) and ($z00$) sites (2·505 and 2·517 Å respectively). Furthermore, in the two sites ($0i0$) and ($z00$) the Ca/Na–O distances are more closely distributed about their average value (σ's of the distributions = 0·15 and 0·14 Å respectively) than for the (000) and ($zi0$) sites (σ = 0·27 and 0·22 Å). This means that the environment of the ($0i0$) and ($z00$) sites is more regular than the other two, and therefore a less marked anisotropy of the Ca/Na atoms is expected. The same geometrical features of the cavities are also common to AnWS, AnQ and BytL (Table 10). For the first two the expected larger anisotropy of thermal parameters in (000) and ($zi0$) sites is verified. For BytL this correlation cannot be checked because the thermal parameters were not refined.

Al–Si *configuration*

Table 11 shows the Al occupancy t for both BytL and BytQ, calculated from $t = (1{\cdot}605 - \langle T{-}O\rangle_{tet}) \times 6{\cdot}58$ (Ribbe & Gibbs, 1969). The Al-rich sites are clearly distinguishable from the Si-rich sites in both structures, but in BytQ the amount of Si present in Al-rich sites, and *vice versa*, is greater than in BytL (the average Al occupancy in Si-rich sites is 0·22 for BytQ and 0·08 for BytL; in Al-rich sites 0·76 for BytQ and 0·82 for BytL), suggesting that at high temperature a certain degree of Si–Al interchange takes place.

To obtain data comparable with the other 7 Å plagioclases, the average Al occupancies over the four T sites related by the pseudosymmetry vectors (**a** + **b** +

Table 10. *Average values and* σ *of the* Ca/Na^{VII}–O *distances and isotropic thermal parameters of the* Ca/Na *atoms in calcic plagioclases*

	(000)				($0i0$)				($z00$)				($zi0$)			
	BytQ	BytL	AnQ	AnWS	BytQ	BytL	AnQ	AnWS	BytQ	BytL	AnQ	AnWS	BytQ	BytL	AnQ	AnWS
Ca/Na–O^{VII}	2·572	2·566	2·574	2·546	2·505	2·524	2·516	2·502	2·517	2·501	2·503	2·490	2·557	2·563	2·564	2·533
σ	0·27	0·24	0·26	0·27	0·15	0·18	0·18	0·15	0·14	0·16	0·14	0·13	0·22	0·24	0·23	0·19
B(Å^2)	3·71	–	3·46	1·20	1·10	–	0·58	0·86	1·08	–	0·78	0·80	5·05	–	3·14	1·43

Table 11. Al-*occupancies* (t) *of the tetrahedral sites in BytQ and BytL*

	BytQ	BytL		BytQ	BytL		BytQ	BytL		BytQ	BytL
t_1(0000)	0·33	0·10	$t_1(m000)$	0·81	0·81	t_2(0000)	0·74	0·69	$t_2(m000)$	0·26	0·02
$t_1(00i0)$	0·17	0·11	$t_1(m0i0)$	0·65	0·78	$t_2(00i0)$	0·75	0·81	$t_2(m0i0)$	0·11	0·15
$t_1(0z00)$	0·67	0·90	$t_1(mz00)$	0·10	0·09	$t_2(0z00)$	0·38	0·11	$t_2(mz00)$	0·64	0·81
$t_1(0zi0)$	1·00	0·95	$t_1(mzi0)$	0·33	0·03	$t_2(0zi0)$	0·02	0·04	$t_2(mzi0)$	0·80	0·84
$\langle t_1(0)\rangle$	0·54	0·52	$\langle t_1(m)\rangle$	0·47	0·43	$\langle t_2(0)\rangle$	0·47	0·41	$\langle t_2(m)\rangle$	0·45	0·46

c)/2 and c/2 are considered (Table 11). Taking into account the standard errors in the average Al occupancy, evaluated from the standard errors in the T–O distances, one can conclude that in both structures there is a significant segregation of Al in $T_1(0)$ sites, while the other three t values are not significantly different from one another. A discrepancy between total Al content given by the chemical analysis (1·85) and that obtained from the t values (1·93) is observed in BytQ. This difference could be attributed to the fact that the absolute values of t calculated by the empirical equation used are not always reliable. Ribbe (1975) proposed a new method for these calculations based on simple proportionation of bond-length differences in which two conditions are imposed: the total Al content is fixed to the value independently evaluated (*e.g.* from the chemical analysis); the three sites $T_1(m)$, $T_2(0)$ and $T_2(m)$ have equal Al occupancy. (This second condition is in agreement with the result previously obtained for BytQ.) The Al occupancies calculated in this way for BytQ and BytL, imposing compositions of An_{85} and An_{80}, are $t_1(0) = 0{\cdot}53$ and $0{\cdot}52$, $t_1(m) = t_2(0) = t_2(m) = 0{\cdot}44$ and $0{\cdot}43$ respectively. These calculations confirm the preferential concentration of Al in the $T_1(0)$ site. The degree of segregation of Al, $\Delta\mathrm{Al} = T_1(0) - [t_1(m) + t_2(0) + t_2(m)]/3$, in $T_1(0)$ with respect to the other three sites is identical in both structures. In conclusion, the thermal treatment at high temperature induces a certain amount of Al–Si diffusion, but does not affect the Al–Si configuration when considered in terms of the four sites of the average structure (for plagioclases of configuration near An_{85}).

Facchinelli & Bruno (1977), studying the variation of cell dimensions of high- and low-calcic plagioclases, observed that only for compositions near An_{85} do γ and γ-related parameters not vary with temperature. Since these parameters are related to the ΔAl (Ribbe, 1975) they predicted that 'the Al concentration in $T_1(0)$ sites in plagioclases of composition near An_{85} is not affected even by extreme thermal treatment'. This appears to be confirmed by the present results, when the average structure is considered.

As seen above, the ΔAl's in BytL and BytQ are the same, in spite of the fact that at temperatures near to T_{solidus} a certain degree of dynamic disorder occurs, consisting of an interchange between Al and Si atoms. This disorder is confirmed by the less pronounced chemical separation between the two main groups of Si-rich and Al-rich sites in BytQ with respect to BytL. To explain the persistent segregation of Al in $T_1(0)$ sites in a structure when Si/Al diffusion occurs, the same kind of hypotheses already proposed for AnQ could be used. In the dynamic equilibrium occurring at high temperatures, the Ca/Na bond strength influences the length of stay of Al and Si in the different tetrahedral sites so that Al will prefer those involving O atoms strongly bonded to Ca/Na atoms. The quenching freezes this dynamic equilibrium and transforms the time average into a space average. The values of the bond-strength sums* from the non-tetrahedral cations received by the O atoms of each average T site are: 0·91, 0·68, 0·80 and 0·72 for $T_1(0)$, $T_1(m)$, $T_2(0)$ and $T_2(m)$ respectively.

It can be seen that for the $T_1(0)$ site the bond-strength contribution from Ca/Na atoms is appreciably larger than those for the other three, even if the correlation between Al occupancy and Ca/Na bond strength is poor. This interpretation of Al occupancy in terms of Ca/Na–O bond strength requires a more detailed analysis of the relationships between the Ca/Na–O and T–O bond strength; the latter depending upon both Al occupancy and linear distortion of tetrahedra. The distortion of tetrahedra, defined as $\Delta_{\text{tet}} = \frac{1}{4}\sum_{i=1}^{4}[(l_i - \bar{l})/\bar{l}]^2$ (Brown & Shannon, 1973), is given for BytQ in Table 7.

As for the discussion of AnQ, the following parameters will be used: (1) $\sum s(\mathrm{Ca/Na{-}O})$: bond-strength sums from Ca/Na atoms; (2) $\sum s(\mathrm{T{-}O})_{\text{in}}$: bond-strength sums from T atoms inside the tetrahedron; (3) $\sum s(\mathrm{T{-}O})_{\text{out}}$: bond-strength sums for T atoms outside the tetrahedron; (4) $\sum s(\mathrm{T{-}O})_{\text{tot}} = \sum s(\mathrm{T{-}O})_{\text{in}} + \sum s(\mathrm{T{-}O})_{\text{out}}$. The summations are extended to the four O atoms of each tetrahedron. Hereinafter, only the four average T sites [$T_1(0)$, $T_1(m)$, $T_2(0)$, $T_2(m)$] will be dealt with, so that there are four values for each parameter, consisting of the average over four single tetrahedra.

The values of the above parameters are calculated in two different ways: (1) With T–O values equal to the average T–O value of each tetrahedron. This procedure implies the assumption of non-distorted tetrahedra. The values so obtained are exclusively related to the Al occupancies and not to the distortion of the tetrahedra. (2) With the actual T–O values obtained in the refinement. In this way the distortion is taken into account. Only the latter procedure leads to values of bond strength meaningful in a discussion of the charge balance. Nevertheless, the differences between the values obtained in the two ways are interesting and helpful in evaluating the way in which the distortions of tetrahedra influence the charge balance. In particular, the differences are always of the same sign for the parameter $\sum s(\mathrm{T{-}O})_{\text{in}}$ because, as a consequence of the slope of the bond-length/bond-strength curve, a bond-strength sum of four T–O of equal length must always be less than a bond-strength sum of four unequal T–O with the same average value. As far as this parameter is concerned the differences are a measure of the spread of the four T–O values within each tetrahedron. As far as $\sum s(\mathrm{T{-}O})_{\text{out}}$ is concerned, the differences can be both positive and negative and depend upon the

* The bond strengths were calculated following Brown & Wu (1976). A linear correction for the Na/Ca substitution was applied.

departure of four T–O bonds belonging to four different tetrahedra from the averages of these four tetrahedra. In Fig. 1(*a*), (*b*), and (*c*) the values of $\sum s(\mathrm{T-O})_{in}$, $\sum s(\mathrm{T-O})_{out}$ and $\sum s(\mathrm{T-O})_{tot}$, calculated in the two different ways, are plotted *versus* $\sum s(\mathrm{Ca/Na-O})$. Fig. 1 shows that: (1) The values of $\sum s(\mathrm{T-O})_{in}$ are mainly controlled by the Al occupancies, even if the distortion significantly influences the trend in such a way as to increase the inverse correlation of this parameter with $\sum s(\mathrm{Ca/Na-O})$ (Fig. 1*a*). (2) The trend of values of $\sum s(\mathrm{T-O})_{out}$ is almost exclusively controlled by the distortions. This effect again operates so as to increase the inverse correlation with $\sum s(\mathrm{Ca/Na-O})$ (Fig. 1*b*). (3) The inverse correlation between $\sum s(\mathrm{T-O})_{tot}$ and $\sum s(\mathrm{Ca/Na-O})$ and the slope of the best-fit curve confirms the achievement of charge balance; this balance is largely obtained by means of the distortions of the tetrahedra, in addition, of course, to the Al occupancies. It should be noted that since this analysis is carried out on a disordered structure and takes into account average situations, the term charge balance is not used in its orthodox meaning of local charge balance (MacKenzie & Smith, 1959).

It would be interesting to examine, in terms of Al occupancies and tetrahedral distortions, the charge-balance trends in the structures of BytL, AnWS and AnQ also. Fig. 1 (*d*) to (*n*) shows, for these structures, the plots of $\sum s(\mathrm{T-O})_{in}$, $\sum s(\mathrm{T-O})_{out}$ and $\sum s(\mathrm{T-O})_{tot}$ *versus* $\sum s(\mathrm{Ca/Na-O})$, already discussed for BytQ. In Table 12 the values of r^2 of the correlations repre-

Table 12. r^2 *values of regression analyses*

Dependent variable: $\Sigma s(\mathrm{Ca/Na-O})$.
Independent variables: $\Sigma s(\mathrm{T-O})$.

	BytQ		BytL		AnQ		AnWS	
	Undistorted	Distorted	Undistorted	Distorted	Undistorted	Distorted	Undistorted	Distorted
$\Sigma s(\mathrm{T-O})_{in}$	0·57	0·82	0·69	0·70	0·99	0·92	0·45	0·55
$\Sigma s(\mathrm{T-O})_{out}$	0·42	0·52	0·52	0·30	0·88	0·85	0·09	0·99
$\Sigma s(\mathrm{T-O})_{tot}$	0·77	0·90	0·50	0·89	0·81	0·99	0·32	0·99

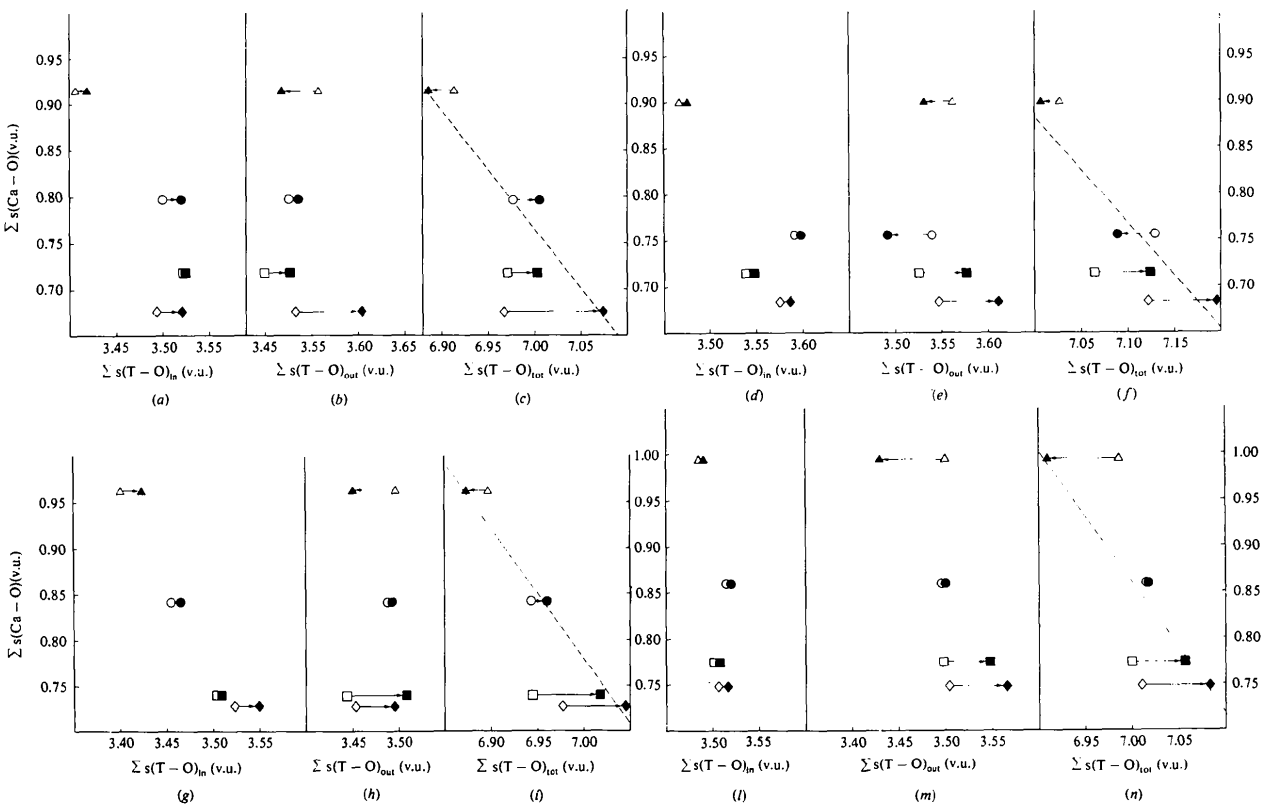

Fig. 1. Ca/Na–O bond-strength sums to the four O atoms of each tetrahedron plotted *versus* T–O bond-strength sums; the T atoms internal to the tetrahedron are considered in (*a*), (*d*), (*g*) and (*l*), the T atoms of neighbouring tetrahedra in (*b*), (*e*), (*h*) and (*m*) and all T atoms in (*c*), (*f*), (*i*) and (*n*). Each point represents the average of the four tetrahedra of the average site: $T_1(0)$ triangles, $T_2(0)$ circles, $T_2(m)$ squares, $T_1(m)$ rhombs. Open symbols: undistorted tetrahedra; filled symbols: actual tetrahedra (see text). (*a*), (*b*), (*c*) plots refer to BytQ, (*d*), (*e*), (*f*) to BytL, (*g*), (*h*), (*i*) to AnQ and (*l*), (*m*), (*n*) to AnWS.

sented in the figures are reported. These plots suggest that: (1) In AnWS, as a straightforward consequence of the Al/Si ratio = 1 and of the perfect alternation Al–Si, the charge-balance trend cannot be influenced by the Al occupancy. The charge balance is merely achieved through the tetrahedral distortion. (2) In AnQ, as already pointed out (Chiari, Facchinelli & Bruno, 1978), the Al occupancy plays a significant role in balancing the different $\sum s$(Ca–O). The representation adopted here allows an evaluation to be made of the significant contribution of the tetrahedral distortion to the charge balance. (3) In BytL again, the two factors cooperate in a way similar to that in BytQ and AnQ.

We thank A. Dal Negro for collecting the X-ray data at Centro di Studio per la Cristallografia Strutturale del CNR, R. Rinaldi and M. G. Vezzalini for the electron-microprobe analysis, L. Pagani for the typing and L. Turco for the drawings. The Consiglio Nazionale delle Ricerche, Roma, Italy, is acknowledged for financing the installation and the maintenance (for the use of all scientists affiliated with Committee 05 of the CNR) of an electron-microprobe laboratory at the Istituto di Mineralogia e Petrologia dell'Università di Modena, whose facilities were used in the present work. This work was supported by CNR Grant 77.00925.

References

ALBEE, A. L. & RAY, L. (1970). *Anal. Chem.* **42**, 1408–1414.

BROWN, I. D. & SHANNON, R. D. (1973). *Acta Cryst.* A**29**, 266–282.

BROWN, I. D. & WU, K. K. (1976). *Acta Cryst.* B**32**, 1957–1959.

BRUNO, E., CHIARI, G. & FACCHINELLI, A. (1976). *Acta Cryst.* B**32**, 3270–3280.

BUSING, W. R., MARTIN, K. O. & LEVY, H. A. (1962). *ORFLS*. Report ORNL-TM-305. Oak Ridge National Laboratory, Tennessee.

CHIARI, G., FACCHINELLI, A. & BRUNO, E. (1978). *Acta Cryst.* B**34**, 1757–1764.

CZANK, M. (1973). *Strukturen des Anorthits bei höheren Temperaturen*. Thesis, ETH, Zürich.

FACCHINELLI, A. & BRUNO, E. (1977). *Rend. Soc. Ital. Mineral. Petrol.* **33**, 152–154.

FLEET, S. G., CHANDRASEKHAR, S. & MEGAW, H. D. (1966). *Acta Cryst.* **21**, 782–801.

FOIT, F. F. & PEACOR, D. R. (1973). *Am. Mineral.* **58**, 665–675.

International Tables for X-ray Crystallography (1968). Vol. III. 2nd ed. Birmingham: Kynoch Press.

JAGODZINSKI, H. & KALUS, C. K. (1977). *Institut Laue–Langevin, Annex to the Annual Report* 1976, p. 130. Grenoble: Dessins.

MACKENZIE, W. S. & SMITH, J. V. (1959). *Acta Cryst.* **12**, 73–74.

MEGAW, H. D., KEMPSTER, C. J. E. & RADOSLOVICH, E. W. (1962). *Acta Cryst.* **15**, 1017–1035.

RIBBE, P. H. (1975). *Feldspars Mineralogy*, edited by P. H. RIBBE, pp. R1–R51. Blacksburg: Southern Printing Co.

RIBBE, P. H. & GIBBS, G. V. (1969). *Am. Mineral.* **54**, 85–94.

WAINWRIGHT, J. E. & STARKEY, J. (1971). *Z. Kristallogr.* **133**, 75–84.

WINTER, J. K., GHOSE, S. & OKAMURA, F. P. (1977). *Am. Mineral.* **62**, 921–931.

ZIEBOLD, T. O. & OGILVIE, R. E. (1964). *Anal. Chem.* **36**, 322–327.

Acta Cryst. (1979). B**35**, 42–45

The Crystal Structures of Manganese(II) Phosphinate Monohydrate, Zinc Phosphinate Monohydrate, and Anhydrous Zinc Phosphinate

BY TIMOTHY J. R. WEAKLEY

Chemistry Department, Dundee University, Dundee DD1 4HN, Scotland

(*Received* 18 *August* 1978; *accepted* 15 *September* 1978)

Abstract

The structures of $Mn(H_2PO_2)_2.H_2O$ [$P2_1/n$, a = 12·013 (16), b = 8·100 (7), c = 13·450 (17) Å, β = 106·28 (3)°, Z = 8; R = 0·080 for 1553 reflections], $Zn(H_2PO_2)_2.H_2O$ [$P2_1/c$, a = 7·692 (6), b = 7·391 (9), c = 10·490 (11) Å, β = 104·15 (4)°, Z = 4; R = 0·051 for 960 reflections], and $Zn(H_2PO_2)_2$ [*Pmma*, a = 6·482 (7), b = 5·363 (4), c = 7·436 (9) Å, Z = 2; R = 0·083 for 302 reflections] have been determined from photographic data. In the monohydrates, which have extended three-dimensional structures, the water molecule is coordinated as well as all anion O atoms, and the MO_6 octahedra are edge-linked in pairs. In $Zn(H_2PO_2)_2$ a layer structure is present, containing chains of edge-linked ZnO_6 octahedra.

0567-7408/79/010042-04$01.00